Immunity, Vol. 12, 495–503, May, 2000, Copyright ©2000 by Cell Press

CCR6 Mediates Dendritic Cell Localization, Lymphocyte Homeostasis, and Immune Responses in Mucosal Tissue

Donald N. Cook,* Dina M. Prosser,* Reinhold Forster,† Jiwen Zhang,* Nelly A. Kuklin,‡ Susan J. Abbondanzo,* Xiao-Da Niu,* Shu-Cheng Chen,* Denise J. Manfra,* Maria T. Wiekowski,* Lee M. Sullivan,* Sidney R. Smith,* Harry B. Greenberg,‡ Satwant K. Narula,* Martin Lipp,† and Sergio A. Lira*§

*Department of Immunology
Schering-Plough Research Institute
Kenilworth, New Jersey 07033
†Max-Delbruck-Center for Molecular Medicine
D-13122 Berlin
Germany
‡Department of Medicine and
Department of Microbiology and Immunology
Stanford University School of Medicine
Stanford, California 94305

Summary

Chemokine-directed migration of leukocyte subsets may contribute to the qualitative differences between systemic and mucosal immunity. Here, we demonstrate that in mice lacking the chemokine receptor CCR6, dendritic cells expressing CD11c and CD11b are absent from the subepithelial dome of Peyer's patches. These mice also have an impaired humoral immune response to orally administered antigen and to the enteropathic virus rotavirus. In addition, *CCR6*$^{-/-}$ mice have a 2-fold to 15-fold increase in cells of select T lymphocyte populations within the mucosa, including CD4$^+$ and CD8$^+$ $\alpha\beta$−TCR T cells. By contrast, systemic immune responses to subcutaneous antigens in *CCR6*$^{-/-}$ mice are normal. These findings demonstrate that CCR6 is a mucosa-specific regulator of humoral immunity and lymphocyte homeostasis in the intestinal mucosa.

Introduction

The vast majority of foreign antigens that contact the body do so at mucosal surfaces, particularly the intestinal mucosa. Lymphocytes in the lamina propria and epithelium of this mucosa are normally tolerant to the large number of luminal antigens present in food and on commensal bacteria, yet they are able to mount a protective humoral and cell-mediated response against enteric pathogens (Shroff et al., 1995). The cellular and molecular basis for this important distinction is not well understood, although it is likely related to several qualitative and quantitative differences between leukocytes in the mucosa and those found in peripheral lymphoid tissues. For example, the intestinal mucosa contains a large number of B lymphocytes that continuously produce and secrete dimerized immunoglobulin (Ig) A into the lumen of the intestine. In addition, the intraepithelial lymphocytes (IEL) of the intestinal mucosa contain several subsets of T lymphocytes, including those bearing the $\gamma\delta$ T cell receptor ($\gamma\delta$−TCR), that are not found in appreciable numbers elsewhere in the body (Goodman and Lefrancois, 1988). Finally, most lymphocytes in the mucosa are activated, a condition which is not seen in other tissues except in inflammatory settings.

Immune responses in mucosal and peripheral lymphoid organs are initiated differently. In the periphery, antigens enter lymph nodes from the lymphatic system, often ferried there by dendritic cells (DC). By contrast, in the small intestine, antigen is acquired directly through the epithelium of Peyer's patches, the lymphoid aggregates embedded in the intestinal wall. Specialized M cells within the Peyer's patch epithelium transport antigen into the underlying subepithelial dome (SED), where mmature DC are thought to take up and process this antigen, undergo maturation, and migrate to T cell–rich interfollicular regions for presentation of the antigen to naive lymphocytes. DC are key mediators of immune responses because they are the only cells that can activate naive lymphocytes (for a recent review, see Banchereau and Steinman, 1998). Different subpopulations of DC may induce different immune responses. DC isolated from Peyer's patches produce IL-10, induce B cell production of IgA, and promote T cell production of cytokines associated with T helper type 2 (Th2) responses, whereas splenic DC induce IgM production and promote T cell production of Th1 associated cytokines (Spalding et al., 1984; Spalding and Griffin, 1986; Everson et al., 1998; Iwasaki and Kelsall, 1999). These different properties of splenic and mucosal DC might contribute to the qualitative differences seen between mucosal and systemic immunity.

Control over immune responses in the intestine is also maintained by differential trafficking patterns of select lymphocyte populations. Naive lymphocytes enter Peyer's patches from the blood through high endothelial venules (HEV). From there, these cells drain via lymphatics to the mesenteric lymph nodes, eventually returning to the general circulation. Lymphocytes activated in Peyer's patches have a predisposition to recirculate, or home, back to the intestinal mucosa. They extravasate from the blood at postcapillary venules within the lamina propria (LP) and establish residence there or in the intestinal epithelium. Thus, they are appropriately positioned to encounter the same type of antigen that was originally presented to them in Peyer's patch. Several families of molecules have been shown to participate in this mucosa-specific homing, including selectins, the immunoglobulin superfamily, and the $\alpha_4\beta_7$ and $\alpha_E\beta_7$ integrins (for reviews see Springer, 1994; Butcher and Picker, 1996).

Another class of molecules, the chemokines, also mediates lymphocyte migration in vivo. The actions of chemokines in vivo have been best studied in inflammatory settings (reviewed in Rollins, 1997), but these molecules

§To whom correspondence should be addressed (e-mail: sergio.lira@spcorp.com).

are also associated with other physiologic processes, including lymphocyte homing (Förster et al., 1996, 1999). The distribution of chemokine receptors varies among different leukocyte populations, providing a potential means by which appropriate leukocyte populations might be selectively recruited during different types of immune or inflammatory responses. However, the assignment of precise biological functions to individual chemokines and their receptors has been complicated by an extensive overlap in the binding of individual chemokines to different chemokine receptors.

An exception to the promiscuous nature of chemokine ligands and receptors is CCR6 (Zaballos et al., 1996), which has only one known ligand, MIP-3α (Rossi et al., 1997), also known as LARC (Hieshima et al., 1997), Exodus (Hromas et al., 1997), and recently given the name of CCL20 in the new chemokine nomenclature system (Zlotnik and Yoshie, 2000). In humans, MIP-3α is expressed in the epithelial crypts of inflamed tonsils and the appendix (Dieu et al., 1998), and in the mouse it is expressed in intestinal epithelium (Tanaka et al., 1999). Human CCR6 expression was originally demonstrated in dendritic cells, spleen, thymus, small intestine, and peripheral blood leukocytes (PBL) (Greaves et al., 1997; Power et al., 1997) and later shown to be expressed in B cells and memory T cells, including $\alpha_4\beta_7$-expressing cells (Liao et al., 1999). The expression patterns of CCR6 and MIP-3α suggest that these molecules might mediate migration of dendritic cells or lymphocytes during systemic or mucosal immune responses.

To investigate the role of CCR6 in vivo, we cloned the murine *CCR6* gene and studied its expression pattern and that of murine MIP-3α. MIP-3α is expressed in the epithelium of Peyer's patches, whereas CCR6 is expressed in a separate but adjacent population of cells within the SED. To investigate the biologic function of CCR6 in Peyer's patch, we generated CCR6-deficient mice (*CCR6*$^{-/-}$) by targeted gene disruption. Analysis of these mice by flow cytometry, immunohistology, and oral immunization studies revealed that CCR6 is a mucosa-specific regulator of humoral immunity and lymphocyte homeostasis in the small intestine.

Results and Discussion

MIP-3α and CCR6 Are Both Expressed in Peyer's Patches

The murine *CCR6* cDNA was cloned from the mouse spleen using a touchdown PCR strategy (Don et al., 1991) that employed degenerate oligonucleotides based on the DNA sequence of the human *CCR6* gene. A portion of the cloned murine *CCR6* gene was used as a probe in Northern blot analysis of 19 different mouse organs. This analysis revealed high levels of *CCR6* mRNA in Peyer's patches, spleen, and lymph nodes, with lower amounts in the thymus, testes, and spinal cord (Figure 1A). This expression profile is generally similar to that previously shown for human CCR6 (Greaves et al., 1997; Power et al., 1997). Analysis of *MIP-3α* mRNA revealed that Peyer's patches are the only tissue in which this chemokine is highly expressed, although lower levels are present in the large intestine and spinal cord. Constitutive MIP-3α expression was previously demonstrated in the thymus of C57BL/6 mice but not of BALB/c mice (Tanaka et al., 1999), suggesting that expression of MIP-3α in the thymus varies depending on mouse strain.

MIP-3α and CCR6 Expressed in Separate but Adjacent Cell Populations

As CCR6 and MIP-3α were both highly expressed in Peyer's patches, we conducted a more detailed analysis of this expression by in situ hybridization. Low magnification of tissue sections showed that MIP-3α is expressed near the boundary of the lumen of the small intestine and Peyer's patch (Figure 1B). Higher magnification revealed that *MIP-3α* mRNA was restricted almost exclusively to the epithelium separating Peyer's patches from the lumen of the small intestine (Figure 1C, note black dots in region marked Ep). Almost no *MIP-3α* mRNA was seen in the underlying subepithelial dome (SED) or in the epithelium associated with the villi of the small intestine. A similar analysis of *CCR6* mRNA revealed that it was also localized near the junction of the intestinal lumen and the Peyer's patch, but in a pattern more diffuse than that seen with MIP-3α (Figure 1D). High magnification revealed that unlike *MIP-3α* mRNA, most of the *CCR6* message was not localized within epithelial cells but rather within the cells of the SED (Figure 1E). Thus, MIP-3α and CCR6 are expressed in separate but adjacent cell populations within the Peyer's patch, suggesting that MIP-3α might have a paracrine function.

Generation and Analysis of CCR6 Homozygous Null Mice

To investigate the biologic function of CCR6 in vivo, we used gene targeting in embryonic stem (ES) cells to generate a deletion encompassing most of the *CCR6* coding region (Figures 2A–2C). Matings between *CCR6* heterozygotes (*CCR6*$^{+/-}$) obtained from ES cell–derived chimeras yielded offspring in a Mendelian proportion of wild-type (*CCR6*$^{+/+}$), *CCR6*$^{+/-}$, and homozygous null (*CCR6*$^{-/-}$) genotypes. The *CCR6*$^{-/-}$ mice appeared healthy and bred well. Northern blot analysis of splenic RNA confirmed that *CCR6* mRNA was absent in the *CCR6*$^{-/-}$ mice (data not shown). In addition, radiolabeled MIP-3α bound to membranes prepared from the spleens of wild-type mice but not to those of *CCR6*$^{-/-}$ mice (Figure 2D). These data confirm that the *CCR6*$^{-/-}$ mice are functionally null for *CCR6* and also demonstrate that no other receptor in the murine spleen binds MIP-3α with high affinity. No gross abnormalities were apparent in any major organs of the *CCR6*$^{-/-}$ mice, and all tissues, including Peyer's patches and the small intestine, appeared normal by light microscopy. There were no baseline differences between *CCR6*$^{-/-}$ and wild-type mice in the number and cellularity of Peyer's patches nor in the relative number of cells in various leukocyte subsets in the spleen, blood, peripheral lymph nodes, thymus, and bone marrow (data not shown). Thus, CCR6 is not required for the development of any major leukocyte populations, including DC, as determined by staining for CD11c, CD11b, and CD8α.

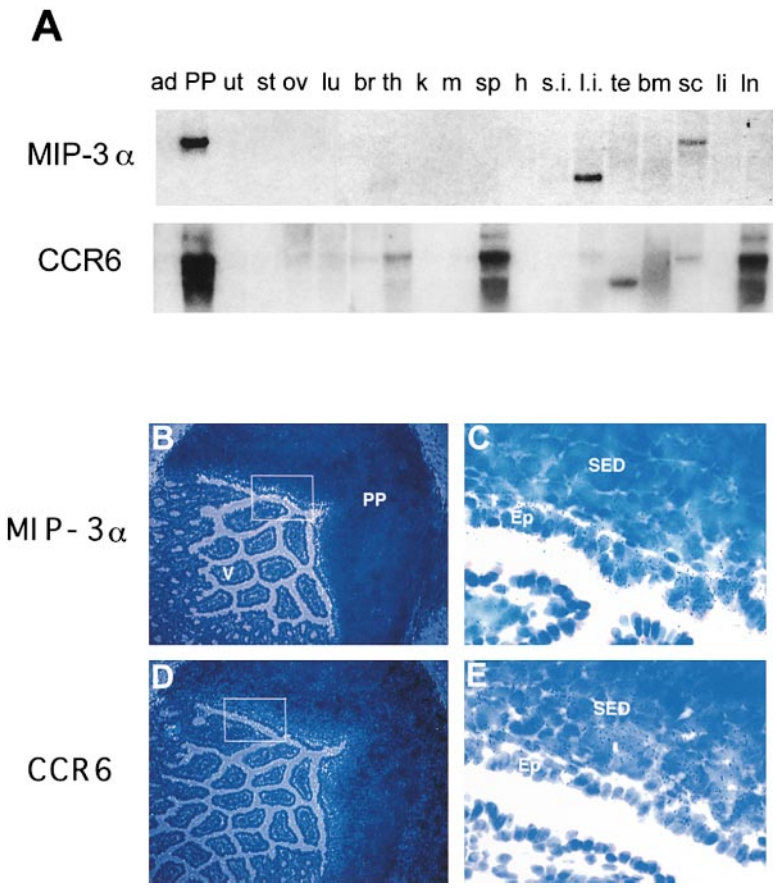

Figure 1. Analysis of CCR6 and MIP-3α Expression in the Mouse

(A) Northern RNA blot of *MIP-3α* (top panel) and *CCR6* (bottom panel) mRNAs. Abbreviations: ad, adrenal; PP, Peyer's patch; ut, uterus; st, stomach; ov, ovary; lu, lung; br, brain; th, thymus; k, kidney; m, skeletal muscle; sp, spleen; h, heart; s.i., small intestine; l.i., large intestine; te, testes; bm, bone marrow; sc, spinal cord; li, liver; ln, lymph nodes. (B–E) In situ hybridization of Peyer's patch with an antisense probe corresponding to MIP-3α (B and C) and CCR6 (D and E). Magnification: (B) and (D), 10×; (C) and (E), 60×. No specific signal was seen with control (sense) probes. Labeled are PP, Peyer's patch; V, villi; SED, subepithelial dome; Ep, epithelium.

Analysis of Dendritic Cells in Peyer's Patch

CCR6 is expressed in immature DC derived from $CD34^+$ bone marrow cells (Dieu et al., 1998). The high expression of MIP-3α in the epithelium of Peyer's patches and of CCR6 in cells of the underlying DC-rich SED suggests that DC might be recruited to the SED by this ligand–receptor pair. To test this possibility, we performed immunohistological analysis of Peyer's patches from *CCR6*$^{-/-}$ mice using antibodies directed against CD11c and CD11b. Antibodies to CD11c detect most types of dendritic cells, and cells staining with antibodies to both CD11c and CD11b represent myeloid-derived DC. In wild-type mice, both $CD11c^+$ $CD11b^-$ (red) and $CD11c^+CD11b^+$ costaining (yellow) cells were seen in the SED (Figure 3A). Examination of *CCR6*$^{-/-}$ mice revealed that although $CD11c^+CD11b^-$ cells were present in the SED, cells staining for both CD11c and CD11b were not detected (Figure 3B). This finding demonstrates that CCR6 expression is required for localization of this DC subset to the SED and suggests that lymphoid epithelium-derived MIP-3α might directly mediate this recruitment.

To determine whether the absence of $CD11c^+CD11b^+$ DC in the SED of *CCR6*$^{-/-}$ mice was associated with other cellular localization or developmental abnormalities in Peyer's patches, we performed additional immunohistologic studies of this tissue. Staining for DEC 205, a molecule found on DC within T cell regions of Peyer's patch and thought to be associated with DC maturation in this tissue (Kelsall and Strober, 1996), did not reveal differences between wild-type mice and *CCR6*$^{-/-}$ mice (Figures 3C and 3D). Similarly, staining for Thy-1 was comparable in both groups of mice, and IgD/IgM staining did not reveal marked abnormalities in germinal center formation of *CCR6*$^{-/-}$ mice (Figures 3E and 3F).

The absence of the $CD11c^+CD11b^+$ DC subset in the SED of Peyer's patches suggested that immune responses and lymphocyte homeostasis might be altered in *CCR6*$^{-/-}$ mice. To test this possibility, we first conducted flow cytometric analyses of cells in the small and large intestine using a panel of antibodies including those directed against B220, CD5, CD45, TCRαβ, TCRγδ, CD4, CD8α, CD8β, Thy1.2, CD69, Gr-1, CD11b, and CD11c. Several statistically significant differences were noted in the epithelium of the small intestine of *CCR6*$^{-/-}$ mice compared to wild-type mice, including a 2-fold increase in the total number of total lymphocytes and T cells as judged by CD45 and Thy1.2 staining, respectively (Figure 4A). This modest increase in total lymphocytes was due to much larger relative increases in several subpopulations of lymphocytes. For example, in the epithelium, activated T cells ($Thy1.2^+CD69^+$) were increased 6-fold, $CD4^+$ cells were increased 9-fold, and $CD4^+CD8^+$ double-positive cells were increased more than 10-fold in *CCR6*$^{-/-}$ mice compared to wild-type mice. Analysis of T cell receptor expression revealed that TCRαβ T cells contribute to the majority of this increase; there was a small increase in TCRγδ cells in

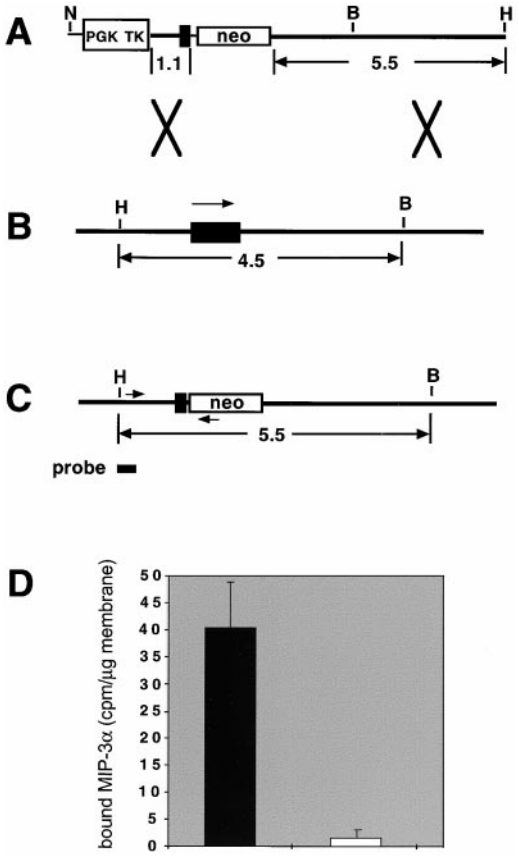

Figure 2. CCR6 Gene Targeting

(A) The targeting construct. The neomycin resistance gene (*neo*) is flanked by a 5.5 kb and a 1.1 kb DNA fragments from the *CCR6* locus.

(B) *CCR6* locus. Restriction sites shown are HindIII (H), BamHI (B), and NotI (N). Sizes are in kilobases. The single *CCR6* exon is shown by a black rectangle and an arrow indicates the direction of transcription.

(C) Structure of the targeted locus. The sizes of the expected fragments are shown in kilobases. Arrowheads represent the primers used in a polymerase chain reaction (PCR) to identify targeted ES cell clones. The probe used for Southern blot confirmation of targeted clones is shown.

(D) Analysis of MIP-3α binding. Radiolabeled MIP-3α was incubated with membranes of splenocytes from wild-type and *CCR6*$^{-/-}$ mice.

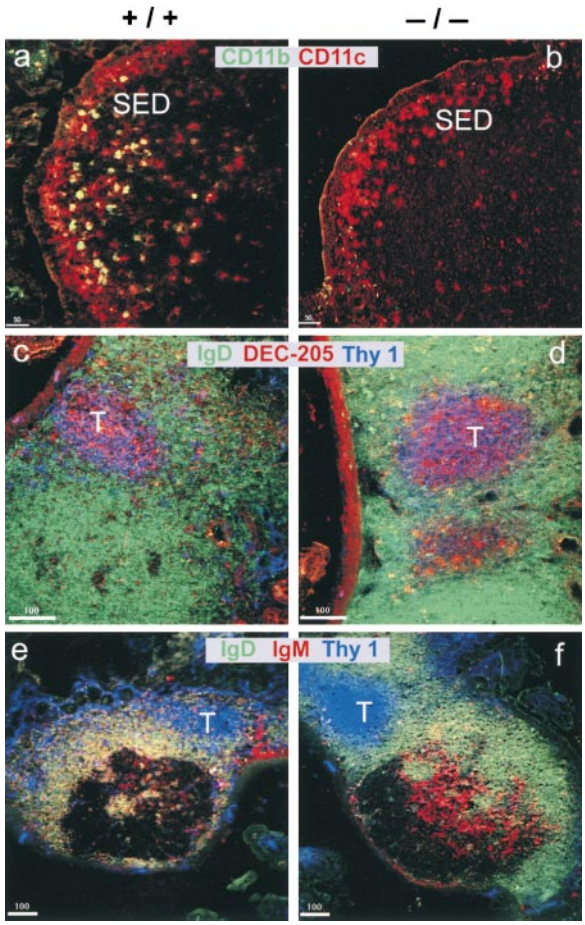

Figure 3. Confocal Analysis of Cell Populations in Peyer's Patch

The antibodies used are as follows: (A and B) CD11b (green) and CD11c (red), double-positive cells stain yellow; (C and D) IgD (green), DEC 205 (red), and Thy-1 (blue); (E and F) IgD (green), IgM (red), and Thy-1 (blue). Wild-type mice, (A, C, E); *CCR6*$^{-/-}$ mice, (B, D, F).

CCR6$^{-/-}$ mice, but this difference was not statistically significant. Similar studies performed with cells prepared from the lamina propria revealed that the number of T lymphocytes were increased in this tissue as well, although the number of B cells as determined by B220 staining was unchanged (Figure 4B). Thus, *CCR6*$^{-/-}$ mice had increases in T lymphocytes within the entire mucosa of the small intestine.

No changes in lymphocyte populations were noted in the mucosa of the large intestine (data not shown). This may be due to the fact that unlike the small intestine, the large intestine does not express high levels of CCR6 (Figure 1A). Analysis of mesenteric lymph nodes revealed that, as seen with the blood, bone marrow, and peripheral lymph nodes, *CCR6*$^{-/-}$ mice did not differ from wild-type mice with regard to TCRαβ cells, CD4^{+} CD8^{+} double-positive cells, or CD8α^{+}β^{+} cells (data not shown). These data suggest that the changes seen in the intestinal mucosa do not result from dysregulated proliferation of these cells outside the mucosa.

Despite the increase in the number of αβ-TCR, CD4^{+}CD8^{+}, and CD8α^{+}β^{+} T cells in the small intestine of *CCR6*$^{-/-}$ mice, no foci of inflammation in the large or small intestine were apparent by light microscopic analysis. To determine the distribution pattern of a lymphocyte population that was overrepresented in the *CCR6*$^{-/-}$ mice, we performed immunohistologic analysis of the small intestine using an anti-CD8β antibody. This antibody was chosen because it recognizes cells expressing the CD8αβ heterodimer but not the CD8α homodimer. These experiments confirmed the increase in CD8α^{+}β^{+} cells seen by flow cytometry and further revealed that these cells were distributed throughout the small intestine in a diffuse pattern (Figure 4C). This low-grade lymphocytic infiltration in the small intestine has some similarities to that seen in humans with celiac disease, or sprue (reviewed recently in Strober and Fuss, 1999), shortly after exposure to the wheat-derived protein gluten. We do not yet know whether the increase in CD8α^{+}β^{+} cells, CD4^{+}CD8^{+} cells, and αβ-TCR cells

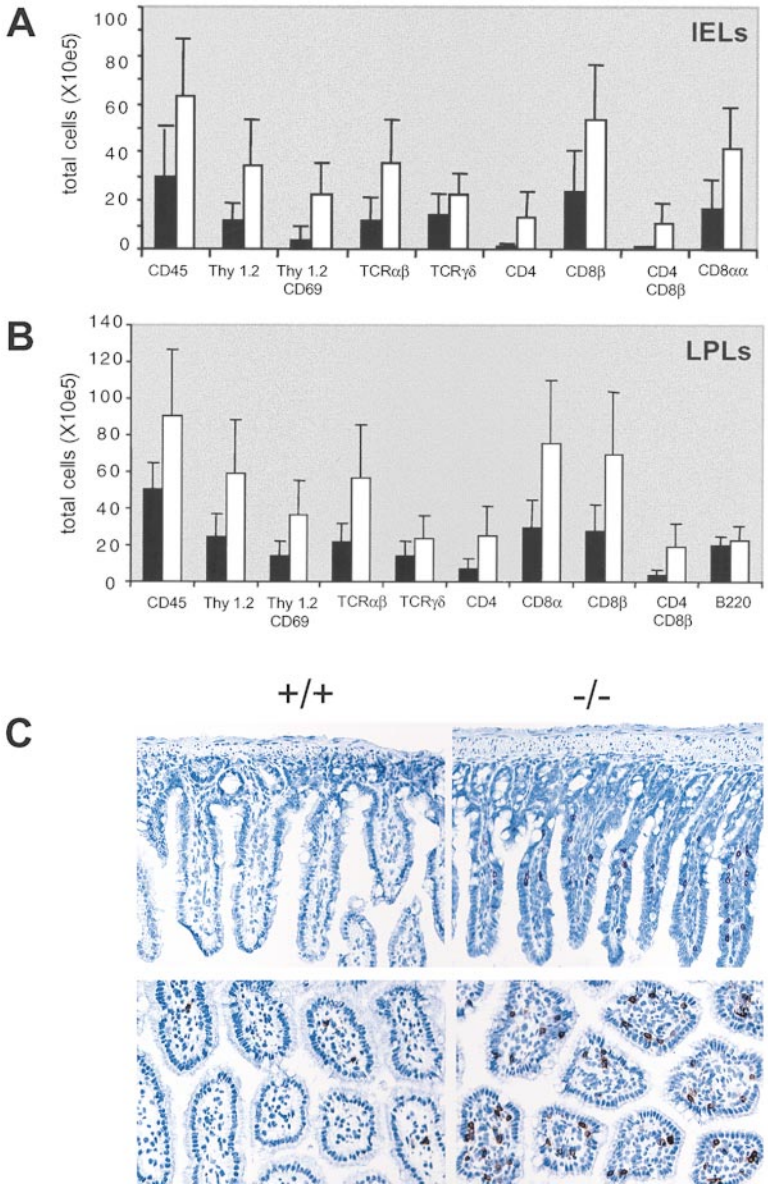

Figure 4. Flow Cytometric Analysis of T Lymphocytes in Intestinal Mucosa

The absolute numbers of the indicated lymphocyte subsets are shown for intestinal epithelium (A) and lamina propria (B). Data shown are representative of a minimum of three experiments. *p* values (two-tailed t test) for all cell populations shown are less than 0.05 except for TCRγδ cells and B220 cells. Wild-type mice, closed rectangles; *CCR6*$^{-/-}$ mice, open rectangles. (C) Immunohistologic staining of CD8β-expressing IEL. Representative longitudinal (top panel) and cross (bottom panel) sections of wild type (+/+) and *CCR6*$^{-/-}$ mice (−/−) are shown.

seen in the *CCR6*$^{-/-}$ mice is associated with the presence of a sensitizing food antigen in their diet.

CCR6$^{-/-}$ Mice Have a Diminished Humoral Response to Orally Administered KLH

The cellular changes seen in both Peyer's patches and the mucosa of *CCR6*$^{-/-}$ mice suggested that CCR6 might function in the immune response in the intestinal mucosa. To test this possibility, we orally immunized wild-type and *CCR6*$^{-/-}$ mice with keyhole limpet hemocyanin (KLH) together with the adjuvant cholera toxin (CT) and measured the number of KLH- and CT-specific antibody-producing cells in Peyer's patches and the lamina propria (Table 1).

CCR6$^{-/-}$ mice had markedly fewer antigen-specific antibody-producing cells than did wild-type mice (Table 1). This reduction was seen both in cells prepared from the lamina propria and in cells prepared from Peyer's patches. Both IgA and IgG isotypes were affected, and similar findings were seen whether KLH- or CT-specific antibody-producing cells were assayed. Thus, the *CCR6*$^{-/-}$ mice have a markedly diminished humoral response to orally administered antigen.

CCR6$^{-/-}$ Mice Have a Normal Systemic Response to Oral and Subcutaneous Antigen

To test the possibility that the diminished humoral response seen in the intestinal mucosa of *CCR6*$^{-/-}$ mice resulted from a general immune defect, we conducted three different experiments. First, we measured the number of KLH-specific antibody-producing cells in the spleens of orally immunized mice (Table 1). The responses of *CCR6*$^{-/-}$ and wild-type mice were indistinguishable in this assay, suggesting that the *CCR6*$^{-/-}$

Table 1. KLH- and CT-Specific Ig-Producing Antibody Cells in Orally Immunized Mice

Antigen-Specific Antibody-Producing Cells/10^6 Cells					
Antigen	Organ	Ig	Wild Type	CCR6$^{-/-}$	*p*
KLH	LP	IgA	121 ± 66	24 ± 5	0.18
KLH	LP	IgG	29 ± 6	11 ± 3	<0.04
KLH	PP	IgA	27 ± 5	6 ± 2	<0.006
KLH	PP	IgG	9 ± 1	2 ± 0.5	<0.002
KLH	Spleen	IgA	6.7 ± 1.5	6.3 ± 3.2	0.88
KLH	Spleen	IgG	5.7 ± 1.5	7.3 ± 2.1	0.33
CT	LP	IgA	1344 ± 202	350 ± 104	<0.003
CT	LP	IgG	307 ± 73	49 ± 20	<0.01
CT	PP	IgA	80 ± 14	26 ± 6	<0.01
CT	PP	IgG	34 ± 4	21 ± 4	<0.05
CT	Spleen	IgA	21 ± 11.8	12 ± 6.2	0.31
CT	Spleen	IgG	17 ± 6.1	19.7 ± 9.1	0.69

A sandwich ELISA using KLH-coated plates was used to detect cells that produce IgA or IgG antibodies specific for KLH or CT. Values represent the mean of five groups of three mice ± standard deviation. *p* values were calculated using the Student's t test.

mice have a normal systemic immune response to orally administered antigen. We also injected KLH subcutaneously and measured levels of total serum Ig and KLH-specific Ig. No differences were seen between wild-type and CCR6$^{-/-}$ mice in total or KLH-specific IgG1, IgG2a, IgG2b, or IgA. Total IgM levels were also unchanged, although increased levels of KLH-specific antibodies were seen in CCR6$^{-/-}$ mice. They also had decreased levels of both total and KLH-specific IgG3 (Figure 5). Finally, in a KLH-induced model of delayed type hypersensitivity, no differences in footpad swelling were seen between *CCR6*$^{-/-}$ and wild-type mice (data not shown). Thus, with the exceptions of IgG3 production, and KLH-specific IgM levels, we did not find marked abnormalities in the systemic immune response to KLH in *CCR6*$^{-/-}$ mice, suggesting that they have a mucosa-specific defect in their humoral response to orally administered antigen.

CCR6$^{-/-}$ Mice Have a Diminished Iga Response to Rotavirus

The diminished humoral response to KLH and the dysregulated lymphocyte population in the intestinal mucosa of the *CCR6*$^{-/-}$ mice suggested that they might also have an impaired response to an enteric pathogen. *CCR6*$^{-/-}$ and wild-type mice were therefore infected with a murine strain of rotavirus, a pathogen that primarily infects the small intestine (Greenberg et al., 1994) and which is responsible for up to a million annual deaths of infants and children worldwide (Glass et al., 1994). Analysis of stools of infected mice revealed that in wild-type mice, rotavirus-specific antibodies were initially produced at significant levels at day 6 postinfection (p.i.), with increasing amounts seen at each day thereafter. *CCR6*$^{-/-}$ mice responded to the infection with similar kinetics, but they had significantly less rotavirus-specific IgA than infected control mice at each time point tested (Figure 6A). The amount of total, nonspecific IgA did not differ between the two groups (data not shown), indicating that the difference in rotavirus-specific antibodies was not due to a general reduction in IgA synthesis in *CCR6*$^{-/-}$ mice. To determine whether the systemic response to rotavirus differed between the two groups of virus-challenged mice, serum levels of anti-rotavirus-specific IgG were assayed. No difference between wild-type mice and *CCR6*$^{-/-}$ mice was seen (Figure 6B). Thus, when orally challenged with either an antigen (KLH) or with a pathogen (rotavirus), the *CCR6*$^{-/-}$ mice had a normal systemic immune response but an impaired mucosal production of antigen-specific IgA.

Delayed Clearance of Rotavirus in *CCR6*$^{-/-}$ Mice

To test whether the reduction in virus-specific IgA in *CCR6*$^{-/-}$ mice was associated with increased levels of rotavirus, stools of infected mice were assayed for the presence of shed virus. No differences between *CCR6*$^{-/-}$ mice and wild-type mice were seen in viral levels during the first 4 days of the infections. However, the *CCR6*$^{-/-}$ mice had a 2-fold increase in virus levels at day 5 ($p < 0.002$) and day 6 ($p < 0.03$) p.i. (Figure

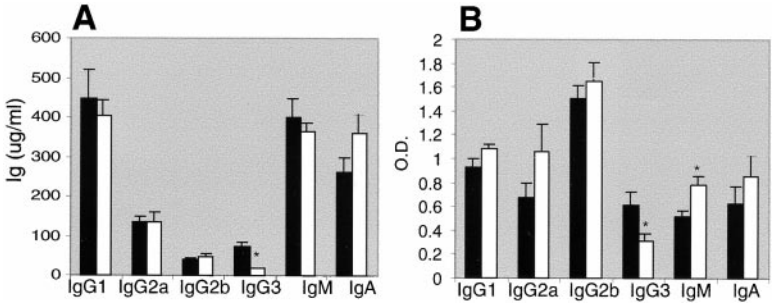

Figure 5. Ig in Serum of KLH-Immunized Mice

Wild-type mice (closed rectangles) and *CCR6*$^{-/-}$ mice (open rectangles) were immunized with KLH, and serum Ig levels determined. (A) Total Ig. (B) KLH-specific Ig. An asterisk denotes differences between wild-type and CCR6$^{-/-}$ mice in which $p < 0.05$.

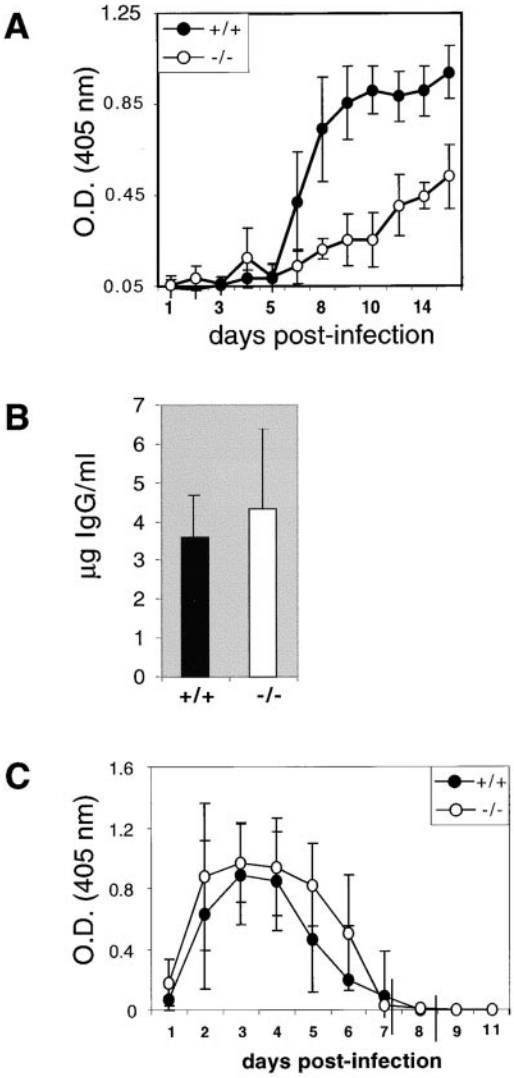

Figure 6. Rotavirus Infection

Mice were infected with 1×10^5 50% diarrhea dose (DD_{50}) of murine rotavirus strain EC and assayed for level of intestinal anti-rotavirus IgA (A), anti-rotavirus serum IgG (B), and rotavirus (C) antigen in stools as previously described (Rosé et al., 1998). Data shown for IgA and IgG is from one of two representative experiments (n = 8/group) having similar results. For antigen, data shown represents pooled results (n = 16/group) of two experiments. Wild-type mice, closed dots and rectangles; *CCR6*$^{-/-}$ mice, open dots and rectangles.

6C), the time at which rotavirus-specific IgA can be detected in stools. Interestingly, B cell–deficient mice that cannot make IgA do not shed excess rotavirus during a primary infection (Franco and Greenberg, 1995) because T cells can also mediate viral clearance. Thus, the increase in viral shedding seen in the *CCR6*$^{-/-}$ mice suggests that CCR6 may have a role in mucosal immunity beyond IgA production.

Taken together, the data presented here demonstrate that CCR6 functions in the humoral response in the intestinal mucosa, and is required for lymphocyte homeostasis in the mucosa of the small intestine. It is not yet clear whether the changes seen in *CCR6*$^{-/-}$ mice result from the loss of function of a single cell type or of multiple cell types. One obvious possibility is that CD11c$^+$CD11b$^+$ DC regulate the immune response of the mucosa, and their absence in the SED of *CCR6*$^{-/-}$ mice is sufficient to result in the changes in lymphocyte populations seen in these mice. This notion is consistent with the finding that compared to DC isolated from the spleen, DC from Peyer's patch produce higher levels of IL-10, promote B cell production of IgA, and induce higher production of Th2-associated cytokines (Iwasaki and Kelsall, 1999). Alternatively, it is possible that the absence of CCR6 on T or B lymphocytes results in defects of activation or migration of these cells, thereby contributing to the changes seen in the mucosa of *CCR6*$^{-/-}$ mice.

In humans, specific phenotypes have been ascribed to individuals having naturally occurring mutations in other chemokine receptor genes, including *CCR5* (Smith et al., 1997) and *DARC* (Horuk et al., 1993). This allelic heterogeneity in human chemokine genes suggests that different human *CCR6* alleles might also exist. If so, it will be of interest to determine whether some of these alleles are associated with an altered mucosal immune function similar to that seen in *CCR6*$^{-/-}$ mice.

Experimental Procedures

Cloning of Murine *CCR6*

A portion of the murine *CCR6* cDNA was cloned from mouse spleen cDNA (Clontech) by a "touchdown" polymerase chain reaction (PCR) strategy using two degenerate primers, 5′-TAYATHGCNATHGT NCA-3′ and 5′-GGRTTNAARCARCARTG-3′. The sequence of these primers was designed based on the sequence of the human *CCR6* gene (Genbank accession number U45984). Cycling conditions were as follows: 7 cycles of 94°C for 1 min, 55°C–43°C annealing for 1 min, decreasing by 2°C per cycle, 72°C for 2 min, followed by 28 cycles of 94°C for 1 min, 55°C annealing for 1 min, and 72° for 2 min.

Gene Targeting

Oligonucleotide primers (5′-GTTGACCGCAGTCACGAGGAGGA-3′ and 5′-CAGGATCGTGATGTCTGTGAGCCA-3′) based on the cloned murine cDNA were used to obtain a bacterial artificial chromosome (BAC) containing the *CCR6* genomic DNA (Genome Systems, St. Louis, MO). An 8 kb fragment bounded by HindIII enzyme recognition sites was subcloned into the pBluescript vector. DNA fragments corresponding to the 5′ and 3′ regions of the *CCR6* locus were in turn subcloned from this plasmid at either end of the neomycin resistance gene (*neo*) contained within the pOSDupDel vector. This targeting vector DNA was linearized using the restriction enzyme NotI prior to its introduction into ES cells by electroporation. DNA from candidate cell lines were initially screened using a PCR strategy using one primer corresponding to the *neo* gene (5′-ACGCGTCACC TTAATATGCG-3′) and another primer corresponding to a region in the *CCR6* locus that is upstream of the 5′ region of homology (5′-GTGCCTTCAGAGGCCAGAATAG-3′). DNAs that yielded the diagnostic PCR product were further analyzed by Southern blotting. DNAs were cleaved with the enzymes HindIII and BamHI, transferred to nylon membranes and hybridized to a radiolabeled DNA probe derived from a region is upstream of the 5′ region of homology. Cells whose DNAs were of the structure predicted for the targeted locus were used to generate chimeric mice using standard blastocyst injection procedures.

MIP-3α Binding Assays

Spleens were washed with ice-cold PBS, homogenized, and debris removed by centrifugation at 10,000 × g. Cell membranes were collected by centrifugation at 100,000 × g and resuspended in PBS to a concentration of 10 mg/ml. Membrane (20 µg) was incubated in a volume of 0.1 ml with 0.05 nM ^{125}I-radiolabeled MIP-3α for 2 hr

at 25°C. The membranes were then filtered through a GF/C filter plate using a Tomtec Harvester, washed with 10 ml PBS, and bound MIP-3α measured by scintillation counting in a Packard microplate counter (TopCount).

Mice

All experiments in which animals were used were conducted in accordance with the institutional guidelines of Schering Plough and Stanford University. Age- and sex-matched 129 SvE × C57BL/6 F2 control mice ($CCR6^{+/+}$) were derived from the same 129 SVE–derived ES cell clone as the $CCR6^{-/-}$ mice and were bred in the same colony under identical conditions.

Northern Blot Analysis

RNA was isolated using RNA STAT-60 reagent (TEL-TEST, Friendswood, TX) according to the manufacturer's specifications. Total RNA was fractionated by agarose formaldehyde gel electrophoresis and transferred to Duralon-UV nylon membranes (Stratagene) according to the manufacturer's protocol. ^{32}P-dCTP (Amersham)-labeled DNA probes were generated from the entire MIP-3α coding regions and from a NdeI fragment containing part of the *CCR6* cDNA by random oligonucleotide-priming using the Prime-It II kit (Statagene). Unincorporated nucleotides were removed using a G-50 spin column (Amersham-Pharmacia), and the probe was hybridized to the membrane-immobilized RNA at 68°C using ExpressHyb buffer (Clontech) according to the manufacturer's specifications.

In Situ Studies

A 228 bp fragment corresponding to the 3′ region of *CCR6* was subcloned into pBluescript ks II. ^{33}P-labeled antisense RNA probes from this region of *CCR6* and from the entire *MIP-3α* cDNA were generated using the Riboprobe Gemini system (Promega, Madison, WI). The probes were hybridized with 10 μM sections of frozen tissue as previously described (Zhang et al., 1997). Slides coated with Kodak NTB2 emulsion were developed after 2 weeks. No signal above background was observed in control hybridization experiments done using sense probes.

Cell Preparations

Fat and Peyer's patches were removed from small intestines, and the fecal contents flushed out with PBS. The intestines were then cut lengthwise to expose the epithelium. Intestines from pools of two mice were washed twice with 30 ml ice-cold calcium- and magnesium-free (CMF) PBS containing 1% fetal calf serum (FCS), then rinsed quickly with cold CMF PBS containing 5% FCS, 5mM EDTA. The preparations were then incubated in 30ml RPMI containing 5% FCS, 5mM EDTA at 37°C for 20 min. After pouring off the supernatant, the intestines were incubated a second time for 20 min at 37°C in 30 ml RPMI containing 5% FCS, 5mM EDTA. The cells contained in the supernatants from both incubations were pooled and poured through a 100 μM nylon mesh, then centrifuged for 15 min at 1000 RPM. This cell pellet was suspended in 3 ml of 1.058 density Percoll solution and overlaid onto 2 ml of 1.103 density Percoll. PBS (2 ml) was layered on top of this. The gradient was centrifuged at 800 rpm for 20 min at room temperature, without brake. Banded cells at the 1.058/1.103 Percoll interface were excised using an 18G needle, dispersed through a 40 μM mesh into 40 ml PBS supplemented with 5% FBS, and centrifuged at 1000 RPM for 10 min. Finally, these cells (IEL) were counted and resuspended at 10^7/ml PBS with 1% BSA, 2% sodium azide.

To isolate LPLs, the intestines from the first two incubations were rinsed in RPMI supplemented with 5% FCS and then incubated twice in RPMI containing 5% FCS, 10 mM HEPES, 1 mM $MgCl_2$, 1.8 mM $CaCl_2$, 0.2 mg/mL collagenase D (Boehringer Mannheim), 1.0 mg/ml hyaluronidase (sigma), and 35 U/ml DNase I (Sigma) for 30 min at 37°C. Supernatants from each incubation were pooled, filtered, centrifuged, banded in Percoll gradients, and collected as described for the preparation of IEL.

Flow Cytometric Analysis

Cells were blocked with 5 μg/ml Fc block (PharMingen), 300 μg/ml mouse IgG (Pierce), and 10% rat serum (Pierce), then stained with PE- or FITC-conjugated monoclonal antibodies directed against CD4, CD8α, CD8β, CD3, CD11c, CD45, B220, Gr-1, NK1.1 TCRαβ, TCRγδ (PharMingen), and DEC-205 (Bachem). Cells were gated on CD45, and data were collected on a FACScan (Becton Dickson) and analyzed using CellQuest software. The total cell number for each population was calculated based on total cells recovered, percentage of CD45 cells, and percentage of CD45-gated cells staining with the various antibodies.

Immunohistology

CD8b staining of the small intestine was done as follows. Fresh frozen 8–10 μm sections were fixed with ice-cold acetone for 10 min and air dried. Sections were blocked with sequential treatment of biotin/avidin blocking kit (Vector, Burlingame, CA), 3% H_2O_2, and 10% normal mouse serum (Vector) for 15 min each. Sections were incubated with anti-CD8b antibody (PharMingen) at 0.5 μg/ml for 1 hr at room temperature, then with a biotinylated mouse anti-rat IgG1/IgG2 (PharMingen) for 30 min, and finally stained using a Vectastain Elite ABC kit (Vector) according to the manufacturer's specifications. All dilutions were done in 1× PBS and 0.1% SDS. Stainings using the antibodies anti-Mac-1 (CD11b)-FITC (10 μg/ml; clone M1/70, PharMingen) anti-CD11c-biotin (10μg/ml; clone HL3, PharMingen), anti-IgD-FITC, anti-IgM-biotin, and Thy-1-Cy5 were performed as previously described (Förster et al., 1999). Biotin was revealed by applying streptavidin-Alexa-Fluor 568 (6μg/ml; Molecular Probes). Signal enhancement of NLDC-145 (DEC-205) mAb was done using the tyramide signal amplification (NEN DuPont).

KLH Oral Immunizations

Fifteen male mice per genotype were gavaged with 3% $NaHCO_3$, 10μg CT (List Biologicals) and 2.5mg KLH (Cal Biochem, CA) in 0.5 ml PBS. Mice were re-immunized in the same manner three more times, with 10 days between immunizations. Six days after the last immunization, lymphocytes were harvested from spleens, Peyer's patches and LP. Cells from groups of 3 animals were pooled and analyzed separately. Cells were plated onto KLH- or CT-coated Millipore 96 well multiscreen filtration plates (HA 0.45μm – MAHA N45 50) in quadruplicate for 3 hr at 37°C, then washed three times with PBS and three times with PBS-0.05% Tween 20. Ten microliters of a 1:500 solution of goat anti-mouse IgA conjugated to horseradish peroxidase was added and incubated 15 hr in a humidified atmosphere. Plates were then washed four times with PBS and incubated with 100 μl/well of 0.4mg/ml 3-amino-9-ethylcarbazole in 50 mM acetate buffer (pH 5.0) containing 0.15% H_2O_2 for 20 min, then washed with H_2O. Spots were counted using a microscope.

Serum Ig Analysis

ELISA assays for total serum Ig levels were run using antibody pairs purchased from PharMingen (San Diego, CA), following the manufacturer's guidelines. Anti-mouse IgM (clone 11/41), anti-mouse IgA (clone R5–140), anti-mouse IgG1 (clone A85–3), anti-mouse IgG2a (clone R11–89), and anti-mouse IgG2b (clone R9–91) were used as capture antibodies. Purified mouse IgM (clone G155–228), IgA (clone M18–254), IgG1 (clone107.3), IgG2a (clone G155–178), and IgG2b (clone 49.2) were used to generate standard curves. Biotin anti-mouse IgM (clone R6–60.2), biotin anti-mouse IgA (clone R5–140), biotin anti-mouse IgG1 (clone A85–1), biotin anti-mouse IgG2a (clone R19–15), and biotin anti-mouse IgG2b (clone R12–3) were used as detection antibodies.

For detection of KLH-specific Ig, mice were immunized with 100 μg of KLH in complete Freund's adjuvant, boosted three weeks later with 100 μg in incomplete Freund's adjuvant, and bled 1 week thereafter. Plates were coated with KLH and blocked, and appropriate dilutions of serum samples were added. After overnight incubation and washing, biotinylated anti-mouse immunoglobulin isotypes (PharMingen) were added. After an additional 2 hr incubation followed by washing, peroxidase-labeled aviden (Sigma) was added, followed by TMB and stop solution (Kirkegaard and Perry). Plates were read at 450 nm and results expressed as OD readings for each group.

Rotavirus Infections

Rotavirus infections were performed and virus and antibody in the stool prepared and analyzed as described previously (Rosé et al.,

1998). The DD_{50} unit is calculated based on the amount of virus required to induce diarrhea in 50% of suckling pups; the viral innoculum used in the present experiments does not cause diarrhea in adult mice.

Acknowledgments

The authors thank Petronio Zalamea, Linda Hamilton, Channa Young, Aparna Subramaniam, Lisa Tardelli, Yuetian Chen, Carol Terminelli, Georgetta Denhardt, Nancy Robertson, Margaret Monahan, Tong-Yuan Yang, and Michael Leach for scientific assistance. We also thank Oliver Smithies, U. of N. Carolina at Chapel Hill, for his gift of the plasmid pOSDupDel. H. B. G. and N. A. K. were supported by a Veteran's Administration merit review grant and National Institutes of Health grant AI 21632.

Received October 21, 1999; revised April 18, 2000.

References

Banchereau, J., and Steinman, R. (1998). Dendritic cells and the control of immunity. Nature *392*, 245–252.

Butcher, E., and Picker, L. (1996). Lymphocyte homing and homeostasis. Science *272*, 60–66.

Dieu, M.-C., Vanbervliet, B., Vicari, A., Bridon, J.-M., Oldham, E., Ait-Yahia, S., Briere, F., Zlotnik, A., Lebecque, S., and Caux, C. (1998). Selective recruitment of immature and mature dendritic cells by distinct chemokines expressed in different anatomic sites. J. Exp. Med. *188*, 373–386.

Don, R., Cox, P., Wainwright, B., Baker, K., and Mattick, J. (1991). "Touchdown" PCR to circumvent spurious priming during gene amplification. Nucleic Acids Res. *25*, 4008.

Everson, M., Lemak, D., McDuffie, D., Koopman, W., McGee, J., and Beagley, K. (1998). Dendritic cells from Peyer's patch and spleen induce different T Helper cell responses. J. Interferon Cytokine Res. *18*, 103–114.

Förster, R., Mattis, E., Kremmer, E., Wolf, E., Brem, G., and Lipp, M. (1996). A putative chemokine receptor, BLR1 directs B cell migration to defined lymphoid organs and specific anatomic compartments of the spleen. Cell *87*, 1037–1047.

Förster, R., Schubel, A., Breitfield, D., Kremmer, E., Renner-Müller, I., Wolf, E., and Lipp, M. (1999). CCR7 coordinates the primary immune response by establishing functional microenvironments in secondary lymphoid organs. Cell *99*, 22–33.

Franco, M., and Greenberg, H. (1995). Role of B cells and cytotoxic T lymphocytes in rotavirus infection. J. Virol. *69*, 7800–7806.

Glass, R., Gentsch, J., and Smith, J. (1994). Rotavirus vaccines: success by reassortment? Science *265*, 1389.

Goodman, T., and Lefrancois, L. (1988). Expression of the γδ receptor on intestinal CD8+ intraepithelial lymphocytes. Nature *333*, 855–858.

Greaves, D., Wang, W., Dairaghi, D., Dieu, M., de Saint-Vis, B., Franz-Bacon, K., Rossi, D., Caux, C., McClanahan, T., Gordon, S., et al. (1997). CCR6, a CC chemokine receptor that interacts with macrophage inflammatory protein 3α and is highly expressed in human dendritic cells. J. Exp. Med. *186*, 837–844.

Greenberg, H., Clark, H., and Offit. (1994). Rotavirus pathology and pathophysiology. In Rotaviruses, R. Ramig, ed. (Berlin: Springer-Verlag), pp. 255–283.

Hieshima, K., Imai, T., Opdenakker, G., Van Damme, J., Kusuda, J., Tei, H., Sakaki, Y., Takatsuki, K., Miura, R., Yoshie, O., and Nomiyama, H. (1997). Molecular cloning of a novel human CC chemokine liver and activation-regulated chemokine (LARC) expressed in liver: chemotactic activity for lymphocytes and gene localization on chromosome 2. J. Biol. Chem. *272*, 5846–5853.

Horuk, R., Chitnis, C., Darbonne, W., Colby, T., Rybicki, A., Hadley, T., and Miller, L. (1993). A receptor for the malarial parasite Plasmodium vivax: the erythrocyte chemokine receptor. Science *261*, 1182–1184.

Hromas, R., Gray, P., Chantry, D., Godiska, R., Krathwohl, M., Fife, K., Bell, G., Takeda, J., Aronica, S., Gordon, M., Cooper, S., Broxmeyer, H., and Klemsz, M. (1997). Cloning and characterization of exodus, a novel β-chemokine. Blood *89*, 3315–3322.

Iwasaki, A., and Kelsall, B. (1999). Freshly isolated Peyer's patch, but not spleen, dendritic cells produce interleukin 10 and induce the differentiation of T helper type 2 cells. J. Exp. Med. *190*, 229–239.

Kelsall, B., and Strober, W. (1996). Distinct populations of dendritic cells are present in the subepithelial dome and T cells regions of the murine Peyer's patch. J. Exp. Med. *183*, 237–247.

Liao, F., Rabin, R., Smith, C., Sharma, G., Nutman, T., and Farber, J. (1999). CC-chemokine receptor 6 is expressed on diverse memory subsets of T cells and determines reponsiveness to macrophage inflammatory protein 3α. J. Immunol. *162*, 186–194.

Power, C., Church, D., Meyer, A., Alouani, S., Proudfoot, A., Clark-Lewis, I., Sozzani, S., Mantovani, A., and Wells, T. (1997). Cloning and characterization of a specific receptor for the novel CC chemokine MIP-3α from lung dendritic cells. J. Exp. Med. *186*, 825–835.

Rollins, B.J. (1997). Chemokines. Blood *90*, 909–928.

Rosé, J., Williams, M., Rott, L., Butcher, E., and Greenberg, H. (1998). Expression of the mucosal receptor α4β7 correlates with the ability of CD8+ memory t cells to clear rotavirus infection. J. Virol. *72*, 4227–4235.

Rossi, D., Vicari, A., Franz-Bacon, K., McClanahan, T., and Zlotnik, A. (1997). Identification through bioinformatics of two new macrophage proinflammatory human chemokines MIP-3α and MIP-3β. J. Immunol. *158*, 1033–1036.

Shroff, K.E., Meslin, K., and Cebra, J.J. (1995). Commensal enteric bacteria engender a self-limiting humoral mucosal immune response while permanently colonizing the gut. Infect. Immunol. *63*, 3904–3913.

Smith, M., Dean, M., Carrington, M., Winkler, C., Huttley, G., Lomb, D., Goedert, J., O'Brien, T., Jacobson, L., Kaslow, R., et al. (1997). Contrasting genetic influence of CCR2 and CCR5 variants on HIV-1 infection and disease progression. Hemophilia growth and development study (HGDS), multicenter AIDS cohort study (MACS), multicenter hemophilia cohort study (MHCS), San Francisco City Cohort (SFCC), ALIVE study. Science *277*, 959–965.

Spalding, D.M., and Griffin, J.A. (1986). Different pathways of differentiation of pre-B cell lines are induced by dendritic cells and T cells from different lymphoid tissues. Cell *44*, 507–515.

Spalding, D.M., Williamson, S.I., Koopman, W.J., and McGhee, J.R. (1984). Preferential induction of polyclonal IgA secretion by murine Peyer's patch dendritic cell-T cell mixtures. J. Exp. Med. *160*, 941–946.

Springer, T. (1994). Traffic signals for lymphocyte recirculation and leukocyte emigration: the multistep paradigm. Cell *76*, 301–314.

Strober, W., and Fuss, I. (1999). Gluten-sensitive enteropathy and other immunologically mediated enteropathies. In Mucosal Immunology, P. Ogra, J. Mestecky, M. Lamm, W. Strober, J. Bienenstock, and J. McGhee, eds. (London: Academic Press), pp. 1101–1128.

Tanaka, Y., Imai, T., Baba, M., Ishikawa, I., Uehira, M., Nomiyama, H., and Yoshie, O. (1999). Selective expression of liver and activation-regulated chemokine (LARC) in intestinal epithelium in mice and humans. Eur. J. Immunol. *29*, 633–642.

Zaballos, A., Varona, R., Gutierrez, J., Lind, P., and Marquez, G. (1996). Molecular cloning and RNA expression of two new human chemokine receptor-like genes. Biochem. Biophys. Res. Commun. *227*, 846–853.

Zhang, J., Zheng, M., Eipper, B.A., and Pintar, J. (1997). Embryonic and uterine expression patterns of peptidylglycine α-amidating monooxygenase transcripts suggest a widespread role for amidated peptides in development. Dev. Biol. *192*, 375–391.

Zlotnik, A., and Yoshi, O. (2000). Chemokines: a new classification system and their role in immunity. Immunity *12*, 121–127.